Research Article Vol. 30, No. 2 / 17 Jan 2022 / Optics Express 1925
Optics EXPRESS

Enhancement of spin noise spectroscopy of rubidium atomic ensemble by using the polarization squeezed light

LELE BAI,[1] LULU ZHANG,[1] YONGBIAO YANG,[1] RUI CHANG,[1] YAO QIN,[1,2] JUN HE,[1,2,3] XIN WEN,[1,4] AND JUNMIN WANG[1,2,3,*]

[1]*State Key Laboratory of Quantum Optics and Quantum Optics Devices, and Institute of Opto-Electronics, Shanxi University, Tai Yuan 030006, China*
[2]*Department of Physics, School of Physics and Electronic Engineering, Shanxi University, Tai Yuan 030006, China*
[3]*Collaborative Innovation Center of Extreme Optics, Shanxi University, Tai Yuan 030006, China*
[4]*Department of Physics, Tsinghua University, Beijing 100084, China*
[*]*wwjjmm@sxu.edu.cn*

Abstract: We measured the spin noise spectroscopy (SNS) of rubidium atomic ensemble with two different kinds of atomic vapor cells (filled with buffer gas or coated with paraffin film on the inner wall) and demonstrated the enhancement of the signal-to-noise ratio (SNR) by using polarization squeezed state (PSS) of 795-nm light field with Stokes operator $\hat{S}_2$ squeezed. The PSS is prepared by locking the relative phase between the squeezed vacuum state of light obtained with a sub-threshold optical parametric oscillator and the orthogonally polarized local oscillator beam by means of the quantum noise lock. Under the same conditions, the PSS can be employed not only to improve the SNR, but also to keep the full width at half maximum (FWHM) of SNS, compared with the case of using the polarization coherent state (PCS), enhancement of SNR is positively correlated with the squeezing level of the PSS. With increasing probe laser power and atomic number density, the SNR and FWHM of SNS will increase correspondingly. With the help of the PSS of the Stokes operator $\hat{S}_2$, quantum improvements of both the SNR and FWHM of SNS signal has been demonstrated by controlling optical power of polarization squeezed light beam or atomic number density in our experiments.

1. Introduction

In any physical system, the inherent random thermal fluctuation and energy change of a certain physical quantity can be reflected when it is measured repeatedly, and the corresponding statistical variation of the average value is called noise. Spin noise (SN) was first proposed by Bloch [1] and verified experimentally by Sleator [2] in the nuclear system, and also was regarded as the random distribution of electron spin under quasi-thermodynamic equilibrium. Spin noise spectroscopy (SNS), is used to reveal a number of capabilities specific to nonlinear optical techniques by changing rotation angle of the far-detuned probe laser's polarization plane, which is manifested as the noise of spin projection on the propagation direction of the probe laser [3]. Aleksandrov and Zapasskii achieved the detection of SNS of the alkali metal vapor cell in an undisturbed manner with a detuning laser [4]. Crooker *et al.* observed the SNS of rubidium and potassium atoms under non-resonant conditions [5]. Horn *et al.* predicted and measured the SNS of rubidium atoms under the condition of resonant optical detection [6]. Ma *et al.* performed a comparative experiment in rubidium atomic vapor cells with different broadening mechanisms [7]. Lucivero *et al.* demonstrated squeezed-light spin noise spectroscopy [8]. Guarrera *et al.* demonstrated that SNS can be used as a versatile technique for the study of noise squeezing in a wide range of spin-based magnetic sensors [9]. Meanwhile, SNS has unique significance in the field of spin

#448084 https://doi.org/10.1364/OE.448084
Journal © 2022 Received 10 Nov 2021; revised 10 Dec 2021; accepted 21 Dec 2021; published 6 Jan 2022

Optics EXPRESS

mechanics of semiconductor nanostructures due to the high content of SN in small spin ensemble, see reviews in Refs. [10,11].

Generally, the physical information contained in SNS under thermal equilibrium must be related to and constrained by the linear response function of the system, such as the signal-to-noise ratio (SNR) of SNS, transverse spin relaxation time of T_2, Lande g_F factor, and etc, which is determined by the wave dissipation theorem [12]. However, the prediction of transverse spin relaxation time can also be used to evaluate its related constraints, which is of great value to the study of optically pumped atomic magnetometer. Calibration of the isotope abundance ratio can be carried out according to the results of SNS [5]; the magnitude of the magnetic field and the nuclear moment can also be calculated accurately by identifying the various peak positions of nonlinear Zeeman results in SNS [13], which will be of potential significance for the performance evaluation of commercial magnetometers. Besides, SNS can also be used to reveal underlying patterns of correlation and coupling beyond linear [14]. The acquisition of the above SNS signals with high quality is the key to obtain information in these fields. Therefore, the measurement of SNS with high SNR and narrow full width at half maximum (FWHM) has potential significance.

However, the squeezed state of light as a special quantum resource, has been widely used in some precision measurement fields, such as gravitational wave detection and magnetic field measurement [15,16]. It also can be described by Stokes operator on Poincare sphere, characterized by the noise of a certain Stokes operator being lower than the standard quantum noise level.The purpose of this work is to apply the 795-nm polarization squeezed state (PSS) with a high squeezing level to detect SNS in two types of rubidium atomic vapor cells to achieve the measurement of SNS with higher SNR and narrower FWHM compared with the case of using the polarization coherence state (PCS) under the same conditions, that is, the quantum enhanced measurement oftechn SNS, which will be helpful to advance the study of the atomic intrinsic properties, and can also be extended to the field of semiconductor materials, such as as resolving controversies about the spin relaxation mechanism of a semiconductor quantum dot qubit [17].

2. Theoretical analysis

An atomic ensemble in thermal equilibrium, with a transverse magnetic field of B perpendicular to the propagation direction of the probe light, is called the Voigt configuration. When the length of atomic vapor cell is L and the cross-sectional area of laser beam is A, the effective total number of atoms is $N = \rho_0 AL$, where ρ_0 represents the atomic number density. Corresponding fluctuation amplitude of magnetization noise in the system is $N^{1/2}$. The basic principle of SNS technique is to project the random spin fluctuations of atoms or the Faraday rotation fluctuation $\langle\theta_F(t)\theta_F(0)\rangle$ induced by magnetization fluctuation $\langle m_Z(t)m_Z(0)\rangle$ onto the linearly polarized probe laser, and can be measured by a balanced polarimeter, shown in Fig. 1(a). When the external transverse magnetic field of B is applied to the atomic ensemble, the probe laser exhibits a random oscillation at the Larmor precession frequency of υ_L, i.e $\upsilon_L = \gamma B$, where γ represents the gyromagnetic ratio of the atomic ground state. SNS can be represented by the magnetic resonance spectrum of the spin system, and the power spectral density in the frequency domain obtained by Fourier transform is $S(\upsilon{>}0) = \int_0^\infty \mathrm{d}t e^{i\upsilon t}\,\langle\theta_F(t)\theta_F(0)\rangle \propto \frac{\Delta\upsilon}{(\upsilon-\upsilon_L)^2+(\Delta\upsilon)^2}$, where $\Delta\upsilon$ is related to laser power (P) and atomic number density (ρ_0), i.e $\Delta\upsilon = \frac{1}{\pi T_2} = \Gamma_0 + \alpha P + \beta\rho_0$[18], Γ_0 represents the atomic spin relaxation rate in the undisturbed state, α represents power broadening factor caused by the interaction of light with atoms, β is collision broadening factor determined by collisions between atoms. Intuitively, we can narrow the FWHM of SNS by reducing the probe laser power and the atomic number density, respectively. In addition, atomic collision broadening can also be weakened by using the spin squeezing [19,20] or an atomic vapor cell coated with with anti-relaxation film, such as octadecyltrichlorosilane (OTS)[21] and paraffin [22] on the inner wall. The above discussion is only applicable to atomic vapor cell with homogeneous broadening

Optics EXPRESS

mechanisms, and the corresponding SNS is a Lorentzian function centered on Larmor precession frequency in the frequency domain, depicted in Fig. 1(b).

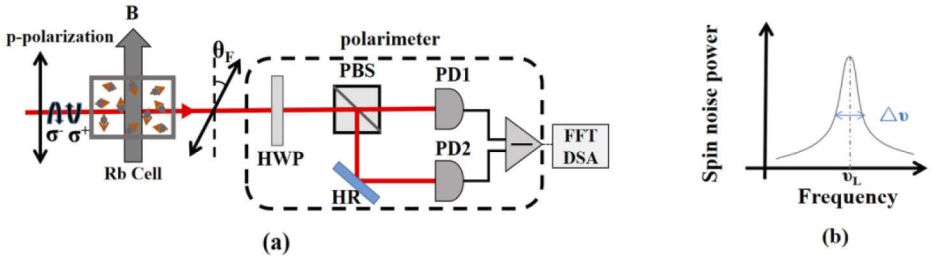

Fig. 1. Schematic diagram for SNS measurement of rubidium atomic ensemble. (a) SNS spectrum can be detected with a balanced polarimeter when a p-polarized laser beam passes through a rubidium atomic vapor cell driven by a transverse magnetic field. To avoid the influence of an external magnetic field, an atomic vapor cell is placed in the center of a multi-layer permalloy (μ-metal) magnetic shielding tank. The linearly p-polarized light beam can be viewed as superposition of left-circularly (σ^+) component and right-circularly (σ^-) polarized component. The random spin noise fluctuation maps the Faraday rotation angle θ_F to the polarization direction of the probe laser beam. (b) SNS spectrum is represented by a Lorentzian curve with a width of $\sim \Delta\upsilon$. The transverse magnetic field of B determines the Larmor precession frequency of υ_L, and the FWHM is determined by the spin's transverse relaxation time T_2. The balanced polarimeter, consisting of a half-wave plate, a polarizing beam splitter cube and two inversely related photo-detectors, is used to reduce laser classical noise and technological noise, and give the final SNS output of differential signal in the measurement of polarization rotation. HWP, half-wave plate; PBS, polarization beam splitter cube; HR, high-reflectivity mirror; PD, photo-electric detector; FFT-DSA, Fast-Fourier-Transform dynamic signal analyzer.

Considering the PCS as the probe laser, the magnitude of the polarization plane rotation output via the polarimeter is characterized by a Fast-Fourier-Transform dynamic signal analyzer (FFT-DSA), and the contribution of the short noise level (SNL) to the final output voltage level is [8]:

$$(\Delta V_{PCS})^2 = (\Delta V_{SNL})^2 = \langle V^2 \rangle_{SNL} = 2G^2 q \Re P \Delta\nu \tag{1}$$

where G is the transimpedance gain of the photo-electric detectors (PDs), q ($q = 1.6 \times 10^{-19} C$) represents the electron charge, $\Delta\upsilon$ is the frequency bandwidth of detectors; $\Re$($\Re = \frac{Qq}{\hbar\omega}$) describes the responsivity of the PDs, which depends on the quantum efficiency of the detectors.

For the PSS, the introduction of the squeezing factor (ξ^2<1) makes the contribution of squeezed photons to the background noise as follows:

$$(\Delta V_{PSS})^2 = \xi^2 (\Delta V_{PCS})^2 \tag{2}$$

and it reduces as the square of the squeezing factor decreases, while the size of other signals to be measured will remain unchanged, resulting in the enhanced SNR.

In SNS measurement, to describe the quality of SNS signal, it is necessary to normalize its noise power and compare it with the SNL. Rubidium atomic ensemble with natural abundance contains two kinds of isotopic atoms,^{85}Rb and ^{87}Rb. The corresponding SNS recorded by FFT-DSA can be fitted by two double-peak Lorentzian functions, see Fig. 2(a), where the left and right peaks represent the SN signals of ^{85}Rb and ^{87}Rb, respectively, and the two analysis frequencies corresponding to two peaks are their respective Larmor precession frequencie The red and blue tracks represent SNS measured by the PCS and the PSS, respectively, and the black dotted line the background noise of the PCS, also known as the SNL.

Optics EXPRESS

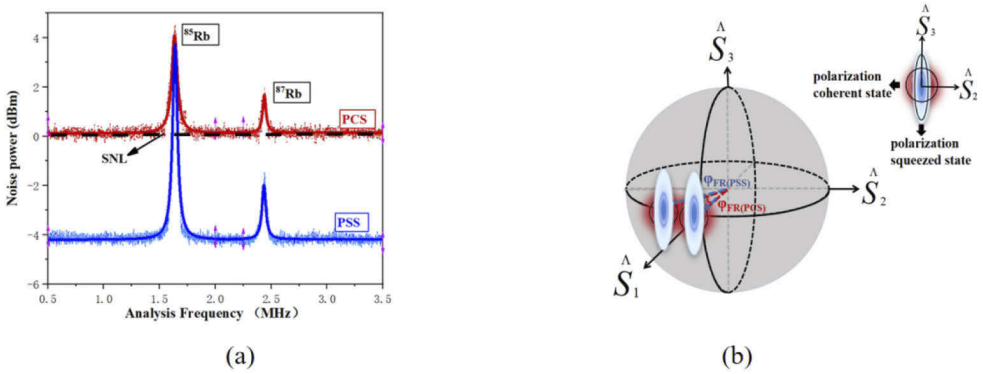

Fig. 2. (a) Models of two light fields (the PCS and the PSS) on Poincare spheres and (b) their measurement results of SNS. SNS signals are measured by the PCS and the PSS. The horizontal and longitudinal coordinates represent the analysis frequency and noise power, respectively. (b) The red sphere represents the PCS state, and its polarization will rotate around the equator and has a rotation angle change of $\varphi_{FR(PCS)}$ in the measurement of SNS. The blue ellipsoid represents the PSS state, in which the Stokes operator $\hat{S}_2$ is squeezed and the Stokes operator $\hat{S}_3$ is anti-squeezed. It produces a rotation angle change of $\varphi_{FR(PSS)}$ under the same condition.

Among them, for the PCS, ξ=1, and for the PSS, 0<ξ<1, shown by the red circle and blue ellipsoid in Fig. 2(b), respectively. For the results of SNS measurement, measured by the PCS and the PSS with the same power, the background noise of the former is higher than that of the latter, while the magnitude of SN remains unchanged. This means that the minimum rotation angle of the polarization plane is more accurate as the noise of the PSS's Stokes operator $\hat{S}_2$ is squeezed, the SNR is improved beyond the SNL.

The magnitude (S_{atom}) of SN is proportional to the atomic number density and square of probe power, and inversely proportional to the effective cross-sectional area A, i.e.

$$S_{\text{atom}} \propto \frac{P^2 \rho_0 L}{A}, \tag{3}$$

the SNR of SNS can be expressed as:

$$SNR = \frac{S_{atom}}{\xi^2 (\Delta V_{PCS})^2} \propto \frac{P \rho_0 L}{\xi^2 A}. \tag{4}$$

It can be seen from Eqs. (3) and (4) that the increase of laser power and atomic number density are beneficial to improve the SNR of the SNS. But they also broaden the FWHM, that is, bring extra power and collision broadening for SNS. Therefore, the trade-off of between these two conditions is particularly important for SNS measurements with high quality, and the introduction of the PSS can solve this issue.

3. Experimental setup

In this experiment, the laser source we used is a continuous-wave narrow-linewidth Ti:sapphire laser (M Squared, Model: Solitis) with a tunable wavelength of 700 -1000 nm and linewidth of 50 kHz, which can satisfy the preparation condition of polarization squeezed light with a high squeezing level at analysis frequency of ~MHz. The experimental device consists of two parts, as shown in Fig. 3 (a): one part is the preparation of the probe laser, which includes the PCS and the PSS (inside the dashed square); and the other part is the establishment of SNS measurement

Optics EXPRESS

system (outside the dashed square). The polarization state of light field can be described by Stokes operatorsPoincare spher, see Fig. 3 (b). In our system, the noise power of Stokes operator $\overset{\Lambda}{S}_2$ of the PSS can be measured by the balanced homodyne detector (BHD) system when the angle between the axis of the half-wave plates (HWP) and the polarization direction of the incident light field is 22.5°. At this point, if a quarter-wave plate (QWP) is placed behind the HWP and the angle set at 45°, then the noise of Stoker operator $\overset{\Lambda}{S}_3$ can be measured [23]. The PSS and the PCS should be focused via a lens before entering atomic vapor cell to make inherent spin fluctuations more relevant and easier to measure. The probe laser with detuning frequency goes straight through the atomic vapor cell along the z direction, which can prevent the atoms from being excited and disturbed. In the case of a focused probe beam, the shape of the SNS is independent of the buffer gas pressure [24].

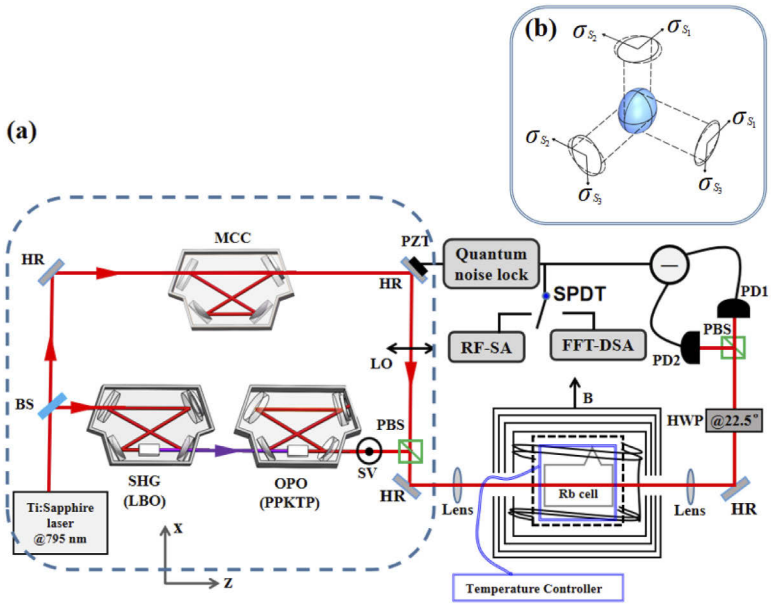

Fig. 3. Experimental setup schematic diagram. The direction of propagation of the probe beam is along z, and the transverse magnetic field is along the direction of x. When the output of OPO is blocked, it means that the probe beam of squeezed vacuum (SV) state from OPO is combined with the LO beam, it represents the PSS as the probe light. The inset (b) represents the noise ellipsoid of the PSS of light prepared in our experiment, which represents tokes operator $\overset{\Lambda}{S}_2$ is squeezed, and Stokes operator $\overset{\Lambda}{S}_3$ is anti-squeezed, and the noise of Stokes operator $\overset{\Lambda}{S}_1$ is at the SNL. The key to figure: BS, beam splitter; SHG, Second harmonic generation; MCC, Mode clean cavity; HR, high-reflectivity mirror; PZT, Piezoelectric transducer; LO, the p-polarized local oscillator beam; SV, the s-polarized squeezed vacuum state; PBS, polarization beam splitter cube; HWP, half-wave plate; RF-SA, the radio-frequency spectrum analyzer; FFT-DSA, the Fast-Fourier-Transformation dynamic signal analyzer; SPDT, single-pole double-throw switch.

A pair of Helmholtz coils that produce a transverse magnetic field and an atomic vapor cell are placed in a four-layer permalloy (μ-metal) magnetic shield. The transverse magnetic field is driven by a precise constant current source (Keysight B2961A). Since the SNS signal is positively correlated with the atomic number density [25,26], the device of non-magnetic heating and

Optics EXPRESS

temperature controller are necessary for the atomic vapor cell to ensure a uniform distribution of atoms, and the heating frequency is 110 kHz.

The magnitude of the SNS signal is determined by the difference in the number of particles spinning up and down in equilibrium, which can result in a Faraday rotation angle of approximately 100 nrads [27,28]. As the rotation signal of the polarization plane is extremely weak and it is difficult to be identified, the same mode background noise (including system inherent noise and classical noise, etc) should be reduced through a balanced polarimeter. In our experimental setup, the detection system can be used not only as a BHD system to measure Stokes operators of the PSS, but also as a (the same function as in Fig. 1(a)) to detect the SNS signal in the form of differential detection, whose differential signal can be amplified and outputed to a radio frequency spectrum analyzer (RF-SA) (Agilent, Model: E4405B) or a FFT-DSA (Zurich Instruments MFLI-5 MHz), respectively. Two orthogonally polarized beams equally divided by a polarization beam splitter (PBS) are focused on two inversely correlated silicon-based detectors with a common mode rejection ratio of 45 dB (at the analysis frequency of ~MHz).

4. Preparation of the PSS of 795-nm light

The preparation of the 795-nm PSS of light mainly consists of four parts: second harmonic generation (SHG), optical parametric oscillator (OPO), local oscillator (LO) beam and quantum noise locking (QNL). To simplify the complexity of the experimental design, generations of the second harmonic, squeezed vacuum (SV) state of the light and LO beam from the same type four-mirror ring cavities, which are independent of each other and have multiple ports for laser injection with great flexibility. For SHG, the nonlinear medium we use is a lithium triborate (LBO) crystal(3 mm×3 mm×13 mm) with critical phase matching, and the efficiency of frequency doubling is high when the power of the fundamental frequency laser is high, even though the nonlinear coefficient is only 0.75 pm/V. Typically, in this experiment, 397.5 nm ultraviolet (UV) laser with power of 380 mW can be generated when power of the 795 nm fundamental frequency is 1 W. For OPO, the crystal is a periodically poled potassium titanyl phosphate crystal (PPKTP) (1 mm×2 mm×15 mm) with a matching method of quasi-phase matching type-0 (e-e + e) and a large nonlinear coefficient of d_{eff} = 7~9 pm/V. However, the transmittance range of wavelengths for PPKTP is from ~350 nm to ~4400 nm, which leads to a particularly severe absorption of 397.5 nm UV-pumped and a large loss of the internal cavity. Hence, the squeezing level of the 795-nm PSS is severely limited compared with the 1064-nm case [29].

The phase matching of the 397.5 nm UV laser beam and the downconversion made of the OPO can be realized with quasi-phase matching and precise temperature control, and the mode clean cavity (MCC) is designed for high quality mode of TEM_{00} output to improve the mode matching with SV. The lengths of all above optical cavities are locked by the Pound-Drever-Hall technique. The noise of squeezed and anti-squeezed state output by OPO can be expressed as [30,31]:

$$R_{\pm} = 1 \pm \eta\varepsilon^2\zeta\rho\frac{4\mathrm{x}}{(1 \mp \mathrm{x})^2 + 4\Omega^2}, \tag{5}$$

where η=94% is the quantum efficiency of the detectors, ε=99.7% represents the interference between SV and LO, ζ=99% is the laser beam's transmission efficiency, ρ=96.6% describes the escape efficiency of the OPO cavity, $x = \sqrt{\frac{P_{pump}}{P_{th}}}$ is the pump parameter, which depends on the UV laser power of P_{pump} and pumping threshold of P_{th}; Ω=0.125 is the tuning parameter in our system, and the estimated pumping threshold P_{th} of the OPO is 206 mW. When the 397.5-nm pump laser power of OPO is 90 mW, the theoretical relative noise power of SV's squeezing and anti-squeezing level normalized to the shot noise level are -7.1 dB and +9.4 dB, respectively. The SV state of light is generated by the sub-threshold OPO, and the corresponding noise power can be measured by scanning the relative phase between the LO beam and the SV [30]. Experimentally,

Optics EXPRESS

the squeezing and the anti-squeezing -5.8 ± 0.2 dB and +7.3 ± 0.2 dB under scanning relative phase are observed at the analysis frequency of 1.63 MHz, as shown in Fig. 4(a).

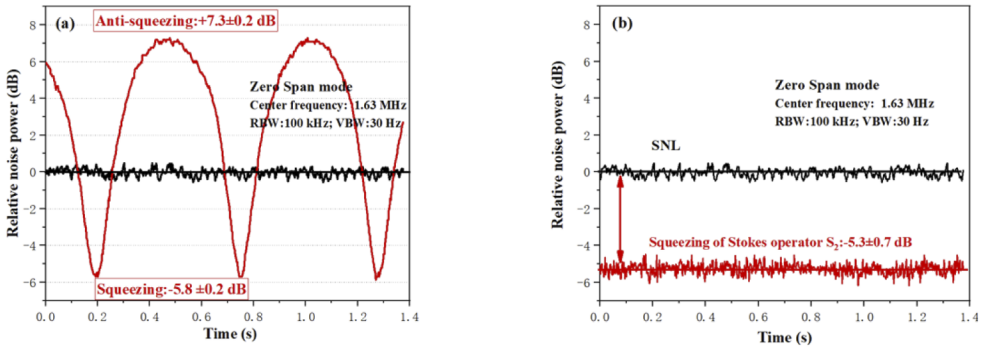

Fig. 4. Relative noise power spectra normalized to the SNL. (a) Preparation of the 795-nm SV state of light. The zero reference line (black) represents the SNL. The red curve represents the relative noise power of SV in the scanning mode of the LO beam's phase, and the maximum squeezing and anti-squeezing are -5.8 ± 0.2 dB and +7.3 ± 0.2 dB, respectively. (b) The noise power of Stokes operator $\hat{S}_2$ relative to the SNL after quantum noise locking. The noise power spectra are measured with an RF-SA (Agilent E4405B) and averaged for 60 times. The RBW is 100 kHz, the VBW is 30 Hz, and the analysis frequency is 1.63 MHz under zero span mode. The Gaussian diameter of the LO beam is 2 mm, and the optical power is 4 mW.

Experimentally, the input laser fields should be continuous PSS of light when it is used as a probe beam in measurement. Synthesizing the SV (s-polarized) and the LO beam (p-polarized) in a certain phase, the PSS of light can be produced [23,32], and its squeezing level is generally lower than the corresponding level measured by scanning mode due to the instability of phase locking. Finally, the squeezing of Stokes operator $\hat{S}_2$ is -5.3 ± 0.7 dB, as shown in Fig. 4(b).

5. Quantum enhanced spin noise spectroscopy

In our experiment, a Pyrex-glass atomic vapor cell with length of $L = 30$ mm and radius of $R = 10$ mm and filled with buffer gas at 10 Torr (Ne) and 20 Torr (He) was used, which can slow down diffusion of atoms to atomic vapor cell's inner wall, thus reducing the destruction of the atomic transverse spin relaxation time. Typically, under the driven of the applied transverse magnetic field of 346.8 μT, and when the atomic number density and the laser power are the same for the PSS and the PCS, corresponding results are shown in Fig. 5(a), which show that the the former can improve the SNR by 3.9 dB compared to the latter without changing the FWHM. The improved level is slightly lower than the squeezing level of the PSS, which is due to from the destruction of the PSS quantum properties after passing through the atomic vapor cell (including the disturbance of high atomic number density, the poor quality of cell windows, and the coupling of thermal noise). Then we measured the SNR and FWHM of SNS results at different powers (0.2 mW-6 mW) (only rubidium 85 atoms are discussed here, because it has a large number of atoms in its natural abundance) when the atomic number density calculated from the vapor pressure curve is $1.48\times10^{11}/\text{cm}^3$ (T = 50°C), as shown in Fig. 5(b), where the black solid squares and red solid circles represent the SNR under measurements using the PCS and the PSS, respectively; the black hollow squares and the red hollow circles represent their respective corresponding FWHM. All the SNR results are improved by at least 3.7 dB (in other words, the signal-to-noise ratio is increased by 2.3 times), and the FWHM is unchanged with the PSS at the same power compared with the PCS. Similarly, as shown in Fig. 5(c) (the graphics

Optics EXPRESS

and color represent the same meaning as Fig. 5(b)), the SNR and FWHM related to the atomic number density (measured from $0.08\times10^{11}/cm^3$(T = 20℃) to $5.36\times10^{11}/cm^3$(T = 65℃)) are obtained keeping the laser power at 3 mW. The SNR is improved by at least 3.7 dB and the FWHM is unchanged with PSS at the same atomic number density compared with the PCS. According to $\Delta\upsilon = \frac{1}{\pi T_2} = \Gamma_0 + \alpha P + \beta\rho_0$, where $\Delta\upsilon$ represents the FWHM, the factors of power broadening(α=3.2 kHz/mW) and atomic collision broadening (β=4.2 kHz/10^{11}cm^{-3}) can be calculated by linearly fitting the corresponding FWHM.

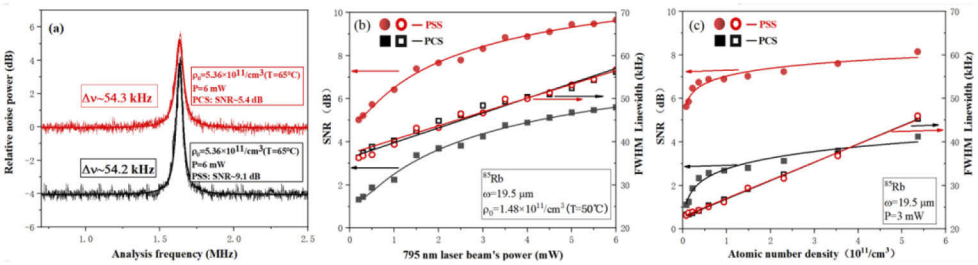

Fig. 5. The SNR and FWHM of SNS are measured by two kinds ofoptical fields in an atomic vapor cell filled with buffer gas at 10 Torr (Ne) and 20 Torr (He). (a) Red line represents the SNS by using the PCS ($\rho_0 = 5.36\times10^{11}/cm^3$, P = 6 mW, SNR = 5.4 dB, Δυ=54.3 kHz). Black line is the result of the PSS ($\rho_0 = 5.36\times10^{11}/cm^3$, P = 6 mW, SNR = 9.1 dB, Δυ=54.2 kHz). The SNS signals are averaged 200 times. (b) $\rho_0 = 1.48\times10^{11}/cm^3$, the SNR (5.0-9.7 dB) detected by the PSS is higher than the results of PCS (1.3-5.6 dB), and the FWHM (36.4 kHz-56.2 kHz) of PSS and PCS are approximately equal under the same laser power. (c) When the probe laser's power is 3 mW, the SNR (5.6 dB-8.2 dB) of the PSS is also higher than the results measured by the PCS (1.1 dB-4.3 dB) under the condition of the same atomic number density, and the FWHM (23.1 kHz-45.3 kHz) of the PSS and the PCS are almost the same. The solid lines are their respective fitting.

Compared with the result in Fig. 5(a), when the power of the PSS is reduced to 3 mW, the corresponding SNR can still be improved by 1.8 dB, and the low bound of the atomic transverse spin relaxation time (T_2) reflected by the FWHM is improved from 5.9 μs (FWHM ~54.3 kHz) to 7.2 μs (FWHM ~44.1 kHz) compared with the PCS, as shown in Fig. 6(a), which benefits from the superiority of quantum enhancement and the reduction of the power broadening. Coincidentally, when the atomic number density measured by the PSS decreases by approximately an order of magnitude, the SNR is improved from ~5.4 dB to ~6.9 dB compared to the PCS case, and the value of T_2 can also be improved from 5.9 μs (FWHM ~ 54.3 kHz) to 6.8 μs (FWHM ~ 46.5 kHz) simultaneously, as shown in Fig. 6(b), which is due to the fact that use of the PSS not only compensates for the undesirable effect of low atomic number density on the SNS signal, but also reduces the severe collision broadening of SNS caused by high atomic number density.

In addition, to obtain SNS with narrower FWHM and to prove the universality of this quantum enhancement effect, we applied this method to another type of atomic vapor cell with a length of $L = 50$ mm and radius of $R = 10$ mm. The inner wall of atomic vapor cell was coated with paraffin film.

Typically, when the transverse magnetic field is 34.6 μT, the corresponding Larmor precession frequency of ^{85}Rb is ~ 163 kHz, and squeezing level of the PSS we used is ~ -3.7 dB due to the coupling of various noises at this analysis frequency [33,34]. To effectively protect the quantum properties of the PSS after passing through the atomic vapor cell and to ensure that the paraffin film on the inner wall is not damaged [35], the temperature of the cell we set is 45 ℃. Finally, we demonstrated that the FWHM was narrowed at the analysis frequency of ~163 kHz, that is, the transverse relaxation time of atomic spins can be well protected. Similarly, use of the PSS can

Optics EXPRESS

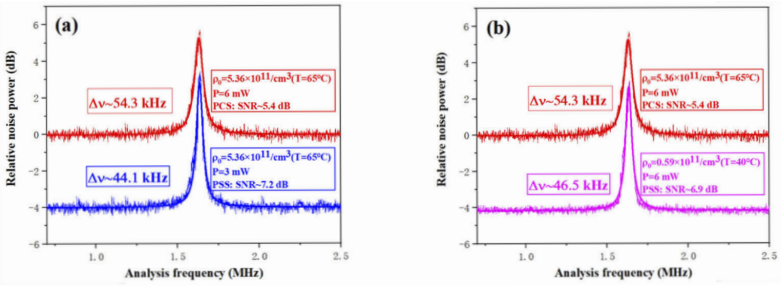

Fig. 6. Rubidium atomic SNS in a vapor cell filled with buffer gas at 10 Torr (Ne) and 20 Torr (He). All signals are for ^{85}Rb atoms. All red lines represent SNS by using the PCS ($\rho_0 = 5.36\times10^{11}/\text{cm}^3$, P = 6 mW, SNR ~ 5.4 dB, $\Delta\upsilon$ ~ 54.3 kHz). (a) The blue line is result of the PSS ($\rho_0 = 5.36\times10^{11}/\text{cm}^3$, P = 3 mW, SNR ~ 7.2 dB, $\Delta\upsilon$ ~ 44.1 kHz). (b) The purple line is result of the PSS ($\rho_0 = 0.59\times10^{11}/\text{cm}^3$, P = 6 mW, SNR ~ 6.9 dB, $\Delta\upsilon$ ~ 46.5 kHz).

still improve the SNR of SNS without changing the FWHM. Typical results are shown in Fig. 7. Under the same condition, when the probe laser power is 1 mW, the atomic number density is $0.94\times10^{11}/\text{cm}^3$, and the SNR can be improved from 2.4 dB to 5.1 dB compared with the case of using the PCS. The the FWHM of ~ 6.2 kHz and corresponding low bound of the atomic transverse spin relaxation time of ~ 51.4 μs can be kept unchanged. According to conclusions obtained in Fig. 5, quantum enhancements of both the SNR and FWHM can also be realized by controlling the laser power of the PSS of light and the atomic number density.

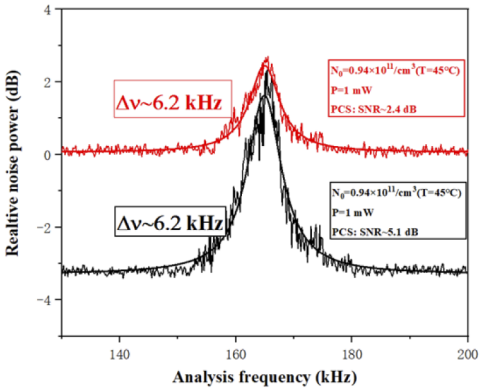

Fig. 7. Stokes-operator squeezed light enhanced rubidium atomic SNS with atomic vapor cell coated with paraffin film on the inner wall. $B = 34.6$ μT. Two SNS signals are for ^{85}Rb atoms, and the red line for the case using the PCS ($\rho_0 = 0.94\times10^{11}/\text{cm}^3$, P = 1 mW, SNR ~ 2.4 dB, $\Delta\upsilon$ ~ 6.2 kHz), whiile the black line for the case using the PSS ($\rho_0 = 0.94\times10^{11}/\text{cm}^3$, P = 1 mW, SNR ~ 5.1 dB, $\Delta\upsilon$ ~ 6.2 kHz). The SNS signals are averaged 200 times.

6. Summary and outlook

The 795-nm PSS with squeezing of -5.3 ± 0.7 dB at the analysis frequency of 1.63 MHz was produced by means of OPO. The results of SNS in two types of rubidium atomic vapor cells are measured via Faraday rotation with the PSS and the PCS respectively, and their SNR and FWHM are positively correlated with laser power and atomic number density. Under the same condition, the PSS has the advantage of surpassing the SNL to increase the SNR without changing the FWHM of SN compared with the PCS case, which demonstrates the quantum enhancement

Optics EXPRESS

properties. Furthermore, PSS can also improve both the SNR and the FWHM simultaneously by appropriately reducing the laser power or atomic number density. These advantages can not only improve measurement accuracy of the intrinsic properties of atomic ensemble, but also play an important role in the semiconductor field.

Although the SN signal is very weak and the SNR is relatively low, however, if SNS magnitude is enhanced by increasing the atomic number density by further heating atomic vapor cell, and if the SNS' linewidth is narrowed by filling the atomic cell with buffer gas at appropriate pressure or coating the cell's inner wall with paraffin film or OTS film against spin relaxation, SNS with higher SNR and narrower FWHM can also be achieved. The SNS with higher SNR and narrower FWHM can be directly applied in transverse magnetic field measurement, even can be used for calibration of commercial fluxgate magnetometers, Hall magnetometer, and etc.

Funding. National Natural Science Foundation of China (11974226, 61905133); National Key Research and Development Program of China (2017YFA0304502); Shanxi Provincial 1331 Project for Key Subjects Construction.

Disclosures. The authors declare no conflicts of interest.

Data availability. Data underlying the results presented in this paper may be available from the corresponding author upon reasonable request.

References

1. F. Bloch, W. W. Hansen, and M. Packard, "The nuclear induction experiment," Phys. Rev. **70**(7-8), 474 (1946).
2. T. Sleator, E. L. Hahn, C. Hilbert, and J. Clarke, "Nuclear-spin noise," Phys. Rev. Lett. **55**(17), 1742 (1985).
3. M. Bogdan, S. A. Crooker, D. G. Rickel, K. B. Blagoev, P. B. Littlewood, and D. L. Smith, "Quantitative study of spin noise spectroscopy in a classical gas of 41K atoms," Phys. Rev. A. **74**(4), 043819 (2006).
4. E. B. Aleksandrov and V.S. Zapasskii, "Magnetic resonance in the Faraday-rotation noise spectrum," Sov. Phys. JETP **54**(1), 132 (1981).
5. S. A. Crooker, D.G. Rickel, A. V. Balatsky, and D. L. Smith, "Spectroscopy of spontaneous spin noise as a probe of spin dynamics and magnetic resonance," Nature **431**(7004), 49 (2004).
6. H. Horn, G. M. Muller, E. M. Rasel, L. Santos, J. Hübner, and M. Oestreich, "Spin-noise spectroscopy under resonant optical probing conditions:Coherent and nonlinear effects," Phys. Rev. A. **84**(4), 043851 (2011).
7. J. Ma, P. Shi, X. Qian, Y. X. Shang, and Y. Ji, "Optical spin noise spectra of Rb atomic gas with homogeneous and inhomogeneous broadening," Sci. Rep. **7**(1), 10238 (2017).
8. V. G. Lucivero, R. Jiménez-Martínez, J. Kong, and M. W. Mitchell, "Squeezed-light spin noise spectroscopy," Phys. Rev. A. **93**(5), 053802 (2016).
9. V. Guarrera, R. Gartman, G. Bevilacqua, and W. Chalupczak, "Spin-noise spectroscopy of a noise-squeezed atomic state," Phys. Rev. Research **3**(3), L032015 (2021).
10. M. Oestreich, M. Römer, R. J. Haug, and D. Hägele, "Spin noise spectroscopy in GaAs," Phys. Rev.Lett. **95**(21), 216603 (2005).
11. F. Berski, H. Kuhn, J. G. Lonnemann, J. Hübner, and M. Oestreich, "Ultrahigh bandwidth spin noise spectroscopy: Detection of large g-Factor fluctuations in highly-n-doped GaAs," Phys. Rev. Lett. **111**(18), 186602 (2013).
12. K. Kubo, "The fluctuation-dissipation theorem," Rep. Prog. Phys. **29**(1), 255 (1966).
13. S. Maheswar, R. Dibyendu, D. Dhanalakshmi, C. Saptarishi, R. Sanjukta, and R. Hema, "Measurements of spin properties of atomic systems in and out of equilibrium via noise spectroscopy," Opt. Express **26**(24), 32168 (2018).
14. P. Glasenapp, N. A. Sinitsyn, D. G. Luyi Yang, D. Rickel, A. Roy, M. Greilich, S. A. Bayer, and Crooker, "Spin noise spectroscopy beyond thermal equilibrium and linear response," Phys. Rev. Lett. **113**(15), 156601 (2014).
15. Y. H. Zhao, N. Aritomi, E. Capocasa, M. Leonardi, M. Eisenmann, Y. F. Guo, E. Polini, A. Tomura, K. Arai, Y. Aso, Y. C. Huang, R. K. Lee, H. Lück, O. Miyakawa, P. Prat, A. Shoda, M. Tacca, R. Takahashi, H. Vahlbruch, M. Vardaro, C. M. Wu, M. Barsuglia, and R. Flaminio, "Frequency-dependent squeezed vacuum source for broadband quantum noise reduction in advanced gravitational-wave detectors," Phys. Rev. Lett. **124**(19), 193002 (2020).
16. B. B. Li, J. Bilek, U. B. Hoff, L. S. Madsen, S. Forstner, V. Prakash, C. Schäfermeier, T. Gehring, W. P. Bowen, and U. L. Andersen, "Quantum enhanced optomechanical magnetometry," Optica **5**(7), 850 (2018).
17. N. A. Sinitsyn and Y. V Pershin, "The theory of spin noise spectroscopy: a review," Rep. Prog. Phys. **79**(10), 106501 (2016).
18. J. Hübner, F. Berski, R. Dahbashi, and M. Oestreich, "The rise of spin noise spectroscopy in semiconductors: From acoustic to GHz frequencies," Phys. Status Solidi **251**(9), 1824 (2015).
19. H Bao, J. L. Duan, S. C. Jin, X. D. Lu, P.X. Li, W. Z. Qu, M. F. Wang, I. Novikova, E. Eugeniy, E. E. Mikhailov, K. F. Zhao, K. Mølmer, H. Shen, and Y. H. Xiao, "Spin squeezing of 10^{11} atoms by prediction and retrodiction measurements," Nature **581**(7807), 159 (2020).
20. D. J. Wineland, J. J. Bollinger, W. M. Itano, and D. J. Heinzen, "Squeezed atomic states and projection noise in spectroscopy," Phys. Rev. A **50**(1), 67 (1994).

Optics EXPRESS

21. Y. J. Tang, Y. Wen, L. Cai, and K. F. Zhao, "Spin-noise spectrum of hot vapor atoms in an anti-relaxation coated cell," Phys. Rev. A. **101**(1), 013821 (2020).
22. Z. G. Wang, X. Peng, R. Zhang, H. Luo, J. J. Li, Z. Q. Xiong, S. S. Wang, and H. Guo, "Single-species atomic comagnetometer based on ^{87}Rb atoms," Phys. Rev. Lett. **124**(19), 193002 (2020).
23. Y. S. Han, X. Wen, J. Y. Liu, J. He, and J. M. Wang, "Generation of polarization squeezed light with an optical parametric amplifier at 795 nm," Opt. Commun. **416**, 1 (2018).
24. V. G. Lucivero, N. D. McDonough, N. Dural, and M. V. Romalis, "Correlation function of spin noise due to atomic diffusion," Phys. Rev. A. **96**(6), 062702 (2017).
25. Z. C. Guo, T. Y. Zhang, and J. Zhang, "Spin noise spectroscopy of cesium vapor in micron-scale cell," Acta Phys. Sin. **69**(3), 037201 (2020), (in Chinese).
26. Y. L. Yang, L. L. Bai, L. L. Zhang, J. He, X. Wen, and J. M. Wang, "Experimental investigation of spin noise spectroscopy of rubidium atomic ensemble," Acta Phys. Sin. **69**(23), 233201 (2020), (in Chinese).
27. M. Römer, J. Hübner, and M. Oestreich, "Spin noise spectroscopy in semiconductors," Rev. Sci Instrum. **78**(10), 103903 (2007).
28. M. Müller, M. Oestreich, M. Römer, and J. Hübner, "Semiconductor spin noise spectroscopy: Fundamentals, accomplishments, and challenges," Physica E. **43**(2), 5697 (2010).
29. S. P. Shi, Y. J. Wang, W. H. Yang, Y. H. Zheng, and K. C. Peng, "Detection and perfect fitting of 13.2 dB squeezed vacuum states by considering green-light-induced infrared absorption," Opt. Lett. **43**(21), 5411 (2018).
30. E. S. Polziki, J. Carri, and H. J. Kimble, "Atomic spectroscopy with squeezed light for sensitivity beyond the vacuum-state limit," Appl. Phys. B. **55**(3), 279 (1992).
31. Y. S. Han, X. Wen, J. He, B. D. Yang, Y. H. Wang, and J. M. Wang, "Improvement of vacuum squeezing resonant on the rubidium D1 line at 795 nm," Opt. Express **24**(3), 2350 (2016).
32. K. Mckenzie, E. E. Mikhailov, K. Goda, P. K. Lam, N. Grosse, M. B. Gray, N. Mavalvala, and D. E. McClelland, "Quantum noise locking," J. Opt. B: Quant.& Semiclass. Opt. **7**(10), S421 (2005).
33. L. L. Bai, X. Wen, Y. L. Yang, J. He, and J. M. Wang, "Laser intensity noise suppression for preparing audio-frequency squeezed vacuum state of light," Appl. Sci. **10**(4), 1415 (2020).
34. X. Wen, Y. S. Han, J. Y. Liu, J. He, Y. H. Wang, and J. M. Wang, "Polarization squeezing at the audio frequency band for the Rubidium D1 line," Opt. Express **25**(17), 20737 (2017).
35. L. L. Bai, X. Wen, Y. L. Yang, L. L. Zhang, J. He, Y. H. Wang, and J. M. Wang, "Quantum-enhanced rubidium atomic magnetometer based on Faraday rotation via 795-nm Stokes operator squeezed light," J. Opt. **23**(8), 085202 (2021).